SIAM REVIEW
Vol. 49, No. 1, pp. 000–000

A Classification of Spikes and Plateaus*

Thomas Hillen†

Abstract. In this paper we classify local maxima into spikes and plateaus. We give analytic definitions for spikes and plateaus in terms of a nonlocal gradient and a fourth order derivative. In higher dimensions the Hesse matrix of $\Delta f(x)$ is of relevance. This classification is applied to pattern formation models in mathematical physics and mathematical biology, including Cahn–Hilliard equations, chemotaxis equations, reaction-diffusion equations, Gierer–Meinhardt models, and Gray–Scott models. We show for some of these examples that the stability of spatial patterns depends on the spike versus plateau type of the solution. We prove, for example, that scalar reaction-diffusion equations in any spatial dimension cannot have stable spike steady states.

AU: See query

Key words. AUTHOR: PLEASE PROVIDE

AMS subject classifications. AUTHOR: PLEASE PROVIDE

DOI. 10.1137/050632427

1. Introduction.

In the current literature on pattern formation of partial differential equations (PDEs) typically two types of patterns are found: "spike" solutions or "plateau" solutions (see, e.g., [14], [12]). Intuitively, spike and plateau patterns can be distinguished easily since spikes are steep local maxima with large curvature at the maximum while plateaus have a broad plane-like maximum with very small curvature. However, no mathematical classification of spikes versus plateaus has been given in the literature. In this paper, the *nonlocal gradient* and the fourth order derivative are used to define *spike* and *plateau* local maxima.

The classification respects the common use of spike and plateau and it is scale invariant. This means that if $f(x)$ has a spike (plateau) at x_0, then $g(\xi) = f(\varepsilon\xi)$ will also have a spike (plateau) at $\xi_0 = x_0/\varepsilon$.

In the one-dimensional case, the analysis is very elementary and could be taught in a beginning calculus class (section 2). For higher dimensions (section 3) some nontrivial tensor calculation is needed, which, however, does not exceed graduate-level mathematics. The primary classification results are stated in Theorems 2.3 and 3.3. Although quite elementary, this distinction of plateaus versus spikes has far reaching consequences. In section 4 it is shown that plateau solutions occur for the Cahn–Hilliard equation, for the volume-filling chemotaxis model, and for the critical domain size problem (details are given later). Spike solutions are typical for the classical chemotaxis model, for Gierer–Meinhardt models, and for Gray–Scott models. It turns out that spikes and plateaus have very different stability properties:

*Received by the editors May 25, 2005; accepted for publication (in revised form) July 11, 2006; published electronically January 30, 2007. This work was supported by NSERC grant G121210825.
http://www.siam.org/journals/sirev/49-1/63242.html

†Mathematical and Statistical Sciences, University of Alberta, Edmonton, AB, T6G 2G1, Canada (thillen@ualberta.ca).

AUTHOR: Please see queries on manuscript page.

1

Write answers on proofs.

For reaction-diffusion equations (section 4.2), for example, we show that typically there are no stable spike steady states. Exceptions can be constructed depending on the boundary conditions (see Theorem 4.2).

For various variants of chemotaxis models we will show in section 4.3 that spike solutions come jointly with finite time blow-up solutions, while the existence of plateau steady states is coupled to global existence of solutions. This fact is very important for biological applications, since blow-up indicates singular behavior of the model that is not observed in nature.

For Gierer–Meinhardt models we will use in section 4.4 the classification of spikes and plateaus to study the stability of two-dimensional stripe patterns. It has been shown by Kolokolnikov et al. [9] that stripe patterns for Gierer–Meinhardt models with saturation (see (4.16)) have no breakup instabilities for a bifurcation parameter b that satisfies $b > b_0 = 0.211376$. Using the classification of spikes and plateaus we will sharpen this estimate for b_0 and show that there are no breakup instabilities if the homoclinic stripe is a plateau ("fat homoclinics" in [9]). This implies an estimate of $b_0 = 0.1961$ (see Theorem 4.8).

For the Gray–Scott model (4.20) we study in section 4.5 the explicit solutions found by Hale, Peletier, and Troy [3]. They showed that homoclinic steady state patterns exist for a parameter γ satisfying $0 < \gamma < \frac{2}{9}$ and $\frac{2}{9} < \gamma < \frac{1}{4}$. For the critical value of $\gamma = \frac{2}{9}$ a pattern made out of two joint heteroclinics appears. Using the classification of spikes versus plateaus we show that this transition is continuous in the sense that the homoclinics change their type close to $\gamma = \frac{2}{9}$. In fact we show that the solution of [3] is a spike for $0 < \gamma < \frac{24}{25}\frac{2}{9}$ and for $0.22938 < \gamma < \frac{1}{4}$ and a plateau for $\frac{24}{25}\frac{2}{9} < \gamma < 0.22938$ (see Theorem 4.11).

2. The One-Dimensional Case. The classification of stripes and plateaus was motivated by a study of nonlocal gradient sensing in chemotaxis models [6]. Chemotaxis denotes the active orientation of moving cells along chemical gradients. These studies generated the idea that a nonlocal gradient might be useful to classify spikes versus plateaus. Consider the schematic in Figure 1. The top row shows a typical spike (a) and a typical plateau (b) with isolated local maximum at x_0. In the second row we plot the corresponding derivatives. For a small value of $\rho > 0$ we compare the slope of the derivative (i.e., the second derivative) with the slope of the straight line connecting $(x-\rho, f(x-\rho))$ to $(x+\rho, f(x+\rho))$ (same with g). It turns out that the straight line connection is less steep than $f''(x_0)$ for a spike, and steeper than $g''(x_0)$ for a plateau. We use this observation for our definitions below.

DEFINITION 2.1. *Let $U \subseteq \mathbb{R}$ be an open domain. For a given Lipschitz continuous function $f : U \to \mathbb{R}$ and for $\rho > 0$, we define a nonlocal gradient as the centered difference for $x \in U$ with $x \pm \rho \in U$ as*

$$\mathring{\nabla}_\rho f(x) := \frac{1}{2\rho}\left(f(x+\rho) - f(x-\rho)\right).$$

Of course, if $f \in C^1(U)$, then $\lim_{\rho\to 0} \mathring{\nabla}_\rho f(x) = f'(x)$. Now we assume that f has an isolated local maximum at $x_0 \in U$ such that

$$f'(x_0) = 0, \quad f''(x_0) < 0. \tag{2.1}$$

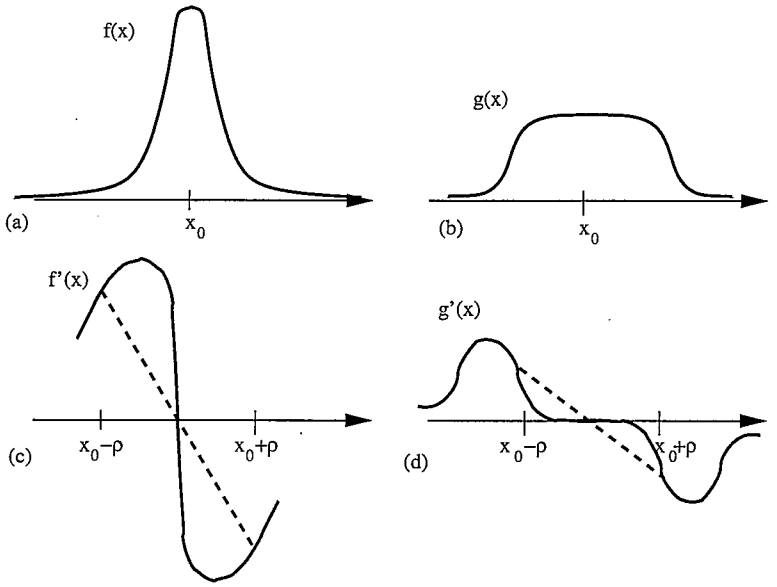

Fig. 1 *Schematic for the definition of spikes and plateaus. In* (a) *a typical spike is shown and in* (c) *we compare the slope of* $f'(x_0)$ *with the nonlocal gradient of* f' *(dashed line). In* (b) *we show a typical plateau and in* (d) *we compare the slope of* $g'(x_0)$ *with the nonlocal gradient of* g' *(dashed line).*

DEFINITION 2.2. *The local maximum* x_0 *is called a*

$$\begin{aligned} \textit{spike} \quad &\Longleftrightarrow \quad \exists\, \rho^* > 0 \quad \textit{such that} \quad 0 > \mathring{\nabla}_\rho f'(x_0) > f''(x_0) \\ &\qquad\quad \textit{for all} \quad 0 < \rho < \rho^*; \\ \textit{plateau} \quad &\Longleftrightarrow \quad \exists\, \rho^* > 0 \quad \textit{such that} \quad 0 > f''(x_0) > \mathring{\nabla}_\rho f'(x_0) \\ &\qquad\quad \textit{for all} \quad 0 < \rho < \rho^*. \end{aligned}$$

We connect these definitions with the fourth order derivative.

THEOREM 2.3. *Assume* $f \in C^5(U)$, x_0 *is a local maximum with* $f'(x_0) = 0$, $f''(x_0) < 0$, *and* $f^{\mathrm{IV}}(x_0) \neq 0$. *Then*

$$\begin{aligned} x_0 \quad &\textit{is a spike} \quad \Longleftrightarrow \quad f^{\mathrm{IV}}(x_0) > 0, \\ x_0 \quad &\textit{is a plateau} \quad \Longleftrightarrow \quad f^{\mathrm{IV}}(x_0) < 0. \end{aligned}$$

Proof. The proof is a straightforward application of Taylor's expansion of $f(x \pm \rho)$. We find

$$\mathring{\nabla}_\rho f'(x_0) = f''(x_0) + \frac{\rho^2}{6} f^{\mathrm{IV}}(x_0) + O(\rho^4).$$

For ρ small enough and $f^{\mathrm{IV}}(x_0) \neq 0$, the sign of $\mathring{\nabla}_\rho f'(x_0) - f''(x_0)$ is given by the sign of $f^{\mathrm{IV}}(x_0)$. □

Remark 2.4. The same classification can be applied for local minima. If x_0 is a local minimum of f, then x_0 is a local maximum of $-f$.

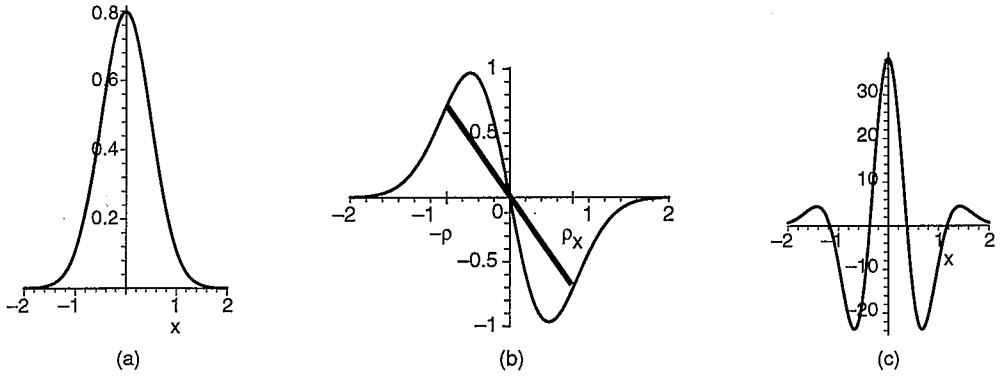

Fig. 2 *The normal distribution,* (a), *and its first and fourth order derivative,* (b), (c). *In* (b) *the nonlocal gradient is sketched as the slope of the straight line.*

Remark 2.5. We see immediately that this classification of spikes and plateaus is scale invariant. If x_0 is a spike (or plateau) for f, then for each $\varepsilon > 0$ the point $\xi_0 = x_0/\varepsilon$ is a spike (or plateau) for $g(\xi) = f(\varepsilon\xi)$.

Example 1. Our standard example of a spike is the normal distribution with mean 0 and variance σ^2:

$$n(x) = \frac{1}{\sigma\sqrt{2\pi}} e^{-\frac{x^2}{2\sigma^2}}.$$

The normal distribution $n(x)$ has a maximum at $x = 0$ and the fourth derivative at 0 is

$$n^{\mathrm{IV}}(0) = \frac{3}{\sigma^5\sqrt{2\pi}},$$

which is always positive and increases as the variance σ^2 decreases. Hence, the maximum is always a spike. In Figure 2(a) the normal distribution is shown with $\sigma = 0.5$. In Figure 2(b) the derivative is shown. The nonlocal gradient for $\rho > 0$ is the slope of the line connecting $(-\rho, n'(-\rho))$ with $(\rho, n'(\rho))$. In Figure 2(b) we see that this line is less steep than the derivative of $n'(0)$, which illustrates the definition of a spike. In Figure 2(c) the fourth order derivative is shown.

Example 2. The standard example for a plateau is cosh. To make the minimum into a maximum, we study

$$h(x) := 20 - \cosh(bx)$$

for some parameter $b > 0$. For the local maximum at $x = 0$ we find

$$h^{\mathrm{IV}}(0) = -b^4.$$

Hence, $h(0)$ is a plateau. In Figure 3(a)–(c) the graph of h, its derivative, and the fourth order derivative are shown. If in the graph of h' (Figure 3(b)) the points $(-\rho, h'(-\rho))$ and $(\rho, h'(\rho))$ were connected by a straight line, then the slope would be steeper than the slope of h' (see definition of plateau).

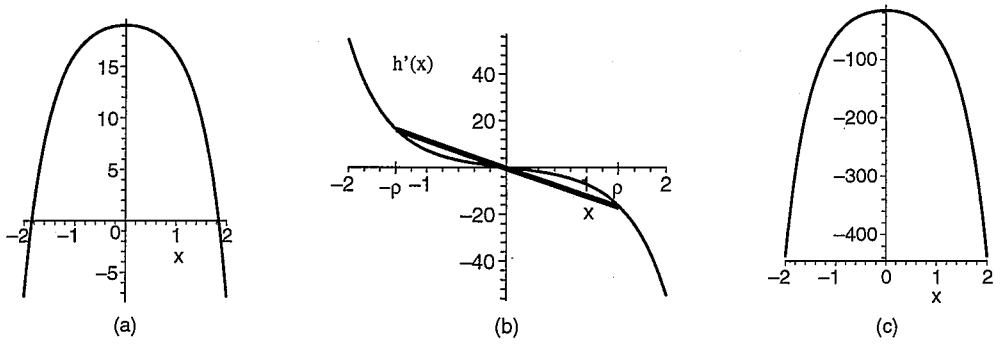

Fig. 3 *The function* $20 - \cosh(2x)$ *is shown in* (a). *The derivative and the fourth order derivative are shown in* (b) *and* (c), *respectively. The nonlocal gradient is shown as slope of the straight line in* (b).

3. Spikes and Plateaus in *n* Dimensions. A similar classification of plateaus and spikes can be given in n dimensions. Let $U \subseteq \mathbb{R}^n$ be an open domain and $f : U \to \mathbb{R}$ a Lipschitz continuous function.

DEFINITION 3.1. *As in Othmer and Hillen* [11], *we define the nonlocal gradient at* $x \in U$ *as an integral over a sphere of radius* $\rho > 0$ *such that* $B_\rho(x) \subset U$ *as*

$$\mathring{\nabla}_\rho f(x) = \frac{n}{w_0 \rho} \int_{S^{n-1}} \sigma f(x + \rho\sigma) d\sigma, \tag{3.1}$$

where $w_0 = |S^{n-1}|$.

This integrated nonlocal gradient has the property that for $f \in C^1(U)$,

$$\lim_{\rho \to 0} \mathring{\nabla}_\rho f(x_0) = \nabla f(x_0),$$

and if $f(x)$ is constant, then $\mathring{\nabla}_\rho f(x_0) = 0$.

Now we assume that $x_0 \in U$ is a local maximum with $\nabla f(x_0) = 0$ and that the Hesse matrix, $\mathrm{Hess}(f(x_0))$, is negative definite. We define plateaus and spikes as in the one-dimensional case.

DEFINITION 3.2. *The local maximum* x_0 *is called a*

$$\begin{aligned} \textit{spike} \quad &\Longleftrightarrow \quad \exists\, \rho^* > 0 \quad \textit{such that} \\ &\quad \mathring{\nabla}_\rho \left(\nabla f(x_0)\right) - \mathrm{Hess}\left(f(x_0)\right) \quad \textit{is positive} \\ &\quad \textit{definite for all} \quad 0 < \rho < \rho^*; \end{aligned}$$

$$\begin{aligned} \textit{plateau} \quad &\Longleftrightarrow \quad \exists\, \rho^* > 0 \quad \textit{such that} \\ &\quad \mathring{\nabla}_\rho \left(\nabla f(x_0)\right) - \mathrm{Hess}\left(f(x_0)\right) \quad \textit{is negative} \\ &\quad \textit{definite for all} \quad 0 < \rho < \rho^*. \end{aligned}$$

By using the n-dimensional Taylor expansion we prove the following classification.

THEOREM 3.3. *Assume* $f \in C^5(U)$ *and* $\mathrm{Hess}\left(\Delta f(x_0)\right)$ *is invertible. Then*

$$x_0 \quad \textit{is a spike} \quad \Longleftrightarrow \quad \mathrm{Hess}\left(\Delta f(x_0)\right) \quad \textit{is positive definite};$$

$$x_0 \quad \textit{is a plateau} \quad \Longleftrightarrow \quad \mathrm{Hess}\left(\Delta f(x_0)\right) \quad \textit{is negative definite.}$$

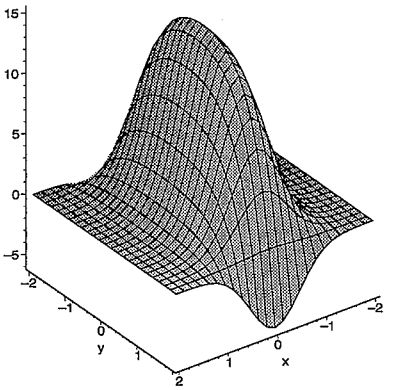

Fig. 4 *Plot of the function* $F(x,y) = \frac{20-\cosh(2y)}{2\sqrt{0.5\pi}} e^{-2x^2}$, *which is spike-like in the* x*-direction and plateau-like in the* y*-direction.*

Remark 3.4. Of course, there are cases of invertible matrices Hess $(\Delta f(x_0))$ that are neither positive nor negative definite. These correspond to local maxima that are spikes in one direction and plateaus in another. Since Hess$(\Delta f(x_0))$ is symmetric, it has a real spectrum, and $\mathbb{R}^n$ can be split into invariant subspaces for positive and for negative eigenvalues. Then the maximum would be spike-like in the eigenspace that corresponds to positive eigenvalues and plateau-like for negative eigenvalues. In Figure 4 we give an example of an x-spike, y-plateau.

Proof of Theorem 3.3. For now we denote $g := \nabla f$ and use tensor notation for the Taylor expansion of g, where summation over repeated indices is assumed:

$$g^j(x+\rho\sigma) = g^j(x) + \partial_k g^j \rho\sigma_k + \partial_k\partial_\ell g^j \frac{\rho^2}{2}\sigma_k\sigma_\ell + \partial_k\partial_\ell\partial_m g^j \frac{\rho^3}{6}\sigma_k\sigma_\ell\sigma_m + O(\rho^4).$$

The nonlocal gradient can be written as

$$\begin{aligned}
\left(\overset{\circ}{\nabla}_\rho (\nabla f)\right)_{ij} &= (\overset{\circ}{\nabla}_\rho\, g^j)_i \\
&= \frac{n}{w_0\rho}\int_{S^{n-1}} \sigma_i\Big(g^j + \sigma_k\rho\partial_k g^j + \sigma_k\sigma_\ell\frac{\rho^2}{2}\partial_k\partial_\ell g^j \\
&\qquad + \sigma_k\sigma_\ell\sigma_m\frac{\rho^3}{6}\partial_k\partial_\ell\partial_m g^j + O(\rho^4)\Big)d\sigma \\
&= \frac{n}{w_0\rho}\Big[\int_{S^{n-1}}\sigma_i d\sigma\; g^j + \rho\int_{S^{n-1}}\sigma_i\sigma_k d\sigma\;\partial_k g^j \\
&\qquad + \frac{\rho^2}{2}\int_{S^{n-1}}\sigma_i\sigma_k\sigma_\ell d\sigma\;\partial_k\partial_\ell g^j \\
&\qquad + \frac{\rho^3}{6}\int_{S^{n-1}}\sigma_i\sigma_k\sigma_\ell\sigma_m d\sigma\;\partial_k\partial_\ell\partial_m g^j \\
&\qquad + O(\rho^4)\Big].
\end{aligned} \tag{3.2}$$

In Hillen [4, Lemma 2.2], a general formula was derived to calculate the directional

tensors $\int_{S^{n-1}} \sigma_i \dots \sigma_m d\sigma$. If we apply Lemma 2.2 of [4], we find

$$\int_{S^{n-1}} \sigma_i d\sigma = 0, \quad \int_{S^{n-1}} \sigma_i \sigma_k \sigma_\ell d\sigma = 0,$$
$$\int_{S^{n-1}} \sigma_i \sigma_k d\sigma = \frac{w_0}{n}\, \delta_{ik},$$
$$\int_{S^{n-1}} \sigma_i \sigma_k \sigma_\ell \sigma_m d\sigma = \frac{w_0}{n(2+n)} \Big(\sum_{P(ik\ell m)} \delta_{ab}\delta_{cd} \Big),$$

where the fourth order index set $P(iklm)$ was explicitly calculated as an example on page 305 of [4] and is given by

$$P(ik\ell m) = \{((i,k)(\ell,m)),\ ((i,\ell),(k,m)),\ ((i,m),(k,\ell))\}.$$

Then

$$\int_{S^{n-1}} \sigma_i \sigma_k \sigma_\ell \sigma_m d\sigma = \frac{w_0}{n(2+n)} \left(\delta_{ik}\delta_{\ell m} + \delta_{i\ell}\delta_{km} + \delta_{im}\delta_{k\ell}\right)$$

and the term (3.2) becomes

$$\begin{aligned} \frac{\rho^3}{6} \int_{S^{n-1}} \sigma_i \sigma_k \sigma_\ell \sigma_m d\sigma\ \partial_k \partial_\ell \partial_m g^j &= \frac{\rho^3 w_0}{6n(2+n)} \left(\partial_i \partial_m \partial_m g^j + \partial_m \partial_i \partial_m g^j + \partial_\ell \partial_\ell \partial_i g^j\right) \\ &= \frac{\rho^3 w_0}{2n(2+n)}\, \partial_i \partial_m \partial_m g^j \\ &= \frac{\rho^3 w_0}{2n(2+n)}\, \partial_i \Delta g^j, \end{aligned}$$

where Δ denotes the Laplace operator. Putting all this together, we find that

$$\left(\mathring{\nabla}_\rho\, (\nabla f)\right)_{ij} = \partial_i g^j + \frac{\rho^2}{2(2+n)}\, \partial_i \Delta g^j + O(\rho^4), \tag{3.3}$$

where we used the fact that the term of order ρ^3 equals zero: $\int_{S^{n-1}} \sigma_i \sigma_j \sigma_k \sigma_\ell \sigma_m d\sigma = 0$ (see Lemma 2.2 in [4]).

In terms of f (3.3) can be written as

$$\mathring{\nabla}_\rho\, (\nabla f) = \text{ Hess}\,(f) + \frac{\rho^2}{2(2+n)}\, \text{Hess}\,(\Delta f) + O(\rho^4). \tag{3.4}$$

In the theorem we assume that Hess $(\Delta f(x_0))$ is invertible. If it is positive (negative) definite, then for ρ small enough, then the matrix $\mathring{\nabla}_\rho\, (\nabla f) -$ Hess (f) is positive (negative) definite as well. If, on the other hand, we know that $\mathring{\nabla}_\rho\, (\nabla f) -$ Hess (f) is positive (negative) definite for ρ small, then the same holds for Hess (Δf). □

4. Examples. In this section we give a number of examples of PDEs where spike or plateau patterns do occur. We begin with an analysis of typical plateau steady states of the Cahn–Hilliard equation. For reaction-diffusion equations we show that typically spikes are unstable. For chemotaxis models we show that spikes are related to finite time blow-up, while plateaus indicate global existence. For Gierer–Meinhardt models we extend the work of Kolokolnikov et al. [9] and show that in two dimensions,

spike-stripes and plateau-stripes have different stability properties. For a Gray–Scott model we show how a heteroclinic pulse is imbedded into a parameter domain of plateau pulses.

In all these examples we study a special but typical case to illustrate the use of the definitions for plateaus and spikes. We do not attempt here to find the most general conditions for the most general model. Detailed biological or physical interpretation of the examples below can be found in the references.

4.1. The Cahn–Hilliard Equation. The classical Cahn–Hilliard equation in one dimension has the form [1]

$$u_t = (-\varepsilon^2 u_{xx} + u^3 - u)_{xx}. \tag{4.1}$$

We consider steady state solutions and assume that at $x_0 \in U \in \mathbb{R}$ we have an isolated local maximum such that $u_x(x_0) = 0$ and $u_{xx}(x_0) < 0$. For now we use prime to denote the partial x-derivative: $u' = u_x$. From (4.1) we find that

$$\varepsilon^2 u^{\mathrm{IV}} = 6u'^2 + 3u^2 u'' - u'',$$

which evaluated at x_0 gives

$$\varepsilon^2 u^{\mathrm{IV}}(x_0) = (3u^2 - 1)u''(x_0).$$

Hence

$$u^{\mathrm{IV}}(x_0) < 0 \quad \text{iff} \quad u(x_0) > \frac{1}{\sqrt{3}}.$$

LEMMA 4.1. *Local maxima x_0 of steady state solutions of the Cahn–Hilliard equation* (4.1) *with $u(x_0) > \frac{1}{\sqrt{3}}$ are plateaus.*

In particular, solutions that are close to 1 are plateaus. We confirm this by looking at a standard approximation of steady states of the Cahn–Hilliard equation given by

$$U(x) = \tanh\left(\frac{x+1}{\varepsilon}\right) + \tanh\left(\frac{1-x}{\varepsilon}\right). \tag{4.2}$$

The fourth order derivative at the local maximum $x_0 = 0$ is

$$U^{IV}(0) = \frac{16\sinh(\varepsilon^{-1})}{\varepsilon^4 \cosh^5(\varepsilon^{-1})}\left(1 - \sinh^2(\varepsilon^{-1})\right),$$

which is of plateau type ($U^{IV}(0) < 0$) for

$$\varepsilon < (\ln(1+\sqrt{2}))^{-1} \approx 1.13.$$

4.2. Reaction-Diffusion Equations. Reaction-diffusion equations are a widely used modeling tool for population dynamics in spatial domains. Here we study an equation for one species in $\Omega \subset \mathbb{R}^n$. If Ω has nonempty boundary in $\mathbb{R}^n$, then we assume $\partial\Omega$ is smooth. The reaction-diffusion model for $u(x,t)$ reads

$$u_t = D\Delta u + f(u), \tag{4.3}$$

with appropriate boundary conditions on $\partial\Omega$.

4.2.1. Unstable Spikes.

THEOREM 4.2. *Assume that a steady state $\bar{u}(x)$ of (4.3) has a local maximum at $x_0 \in \Omega$ of spike type. Then*

$$f'(\bar{u}(x_0)) > 0.$$

Moreover, let $\mu_0 \leq 0$ denote the leading eigenvalue of the Laplacian Δ on Ω with the corresponding boundary conditions. If

$$\mu_0 > -\frac{f'(\bar{u}(x_0))}{D},$$

then this spike is linearly unstable.

Proof. We assume that a steady state $\bar{u}(x)$ has a local maximum at x_0 satisfying $\nabla\bar{u}(x_0) = 0$ and $\mathrm{Hess}(\bar{u}(x_0))$ is negative definite. Using the reaction-diffusion equation (4.3) for steady states we find that

$$\mathrm{Hess}(\Delta\bar{u}(x_0)) = -f'(\bar{u}(x_0))\ \mathrm{Hess}(\bar{u}(x_0)).$$

Since we assume that x_0 is a spike, we know that $\mathrm{Hess}(\Delta\bar{u}(x_0))$ is positive definite. Since $\mathrm{Hess}(\bar{u}(x_0))$ is negative definite it follows that $f'(\bar{u}(x_0)) > 0$.

Linearization of the reaction-diffusion equation (4.3) at the steady state $\bar{u}(x)$ gives for a small perturbation $\eta(x,t) = u(x,t) - \bar{u}(x)$ the equation

$$\eta_t = D\Delta\eta + f'(\bar{u})\eta.$$

A necessary condition for stability is that the leading eigenvalue μ_0 satisfies

$$D\mu_0 < -f'(\bar{u}(x)) \quad \text{for all } x \in \Omega. \tag{4.4}$$

Hence if this condition (4.4) is violated at at least one point x_0, then the spike is unstable. □

Remark 4.3. If the domain or boundary conditions are such that $\mu_0 = 0$ is the leading eigenvalue, then spikes can never be stable. This includes, for example, $\Omega = \mathbb{R}^n$, or rectangular domains Ω with homogeneous Neumann boundary conditions or with periodic boundary conditions.

Remark 4.4. The opposite result, that plateaus are always stable, must not be true, since in that case we need to show that condition (4.4) holds for all $x \in \Omega$. The classification of plateaus gives us only information about x_0. Instabilities of plateaus might occur at the transition layers that are not close to x_0.

4.2.2. The Critical Patch-Size Problem. The critical patch-size problem is a classical problem in mathematical ecology [13] . It refers to the question of whether the classical Fisher equation on a bounded interval $[0,\ell]$ with Dirichlet boundary conditions supports nontrivial steady states. The model is given as

$$u_t = Du_{xx} + \mu u\left(1 - \frac{u}{K}\right),$$
$$u(0,t) = 0, \quad u(\ell,t) = 0.$$

It is well known (see, e.g., de Vries et al. [2]) that steady states are solutions of the following Hamilton system:

$$u' = v, \qquad v' = -\frac{\mu}{D}u\left(1 - \frac{u}{K}\right). \tag{4.5}$$

Nontrivial steady states have a unique maximum at $x = \ell/2$ with $0 < u(\ell/2) < K$. We find that

$$u^{\mathrm{IV}}(\ell/2) = \frac{\mu^2}{D^2}\left(1 - \frac{2u(\ell/2)}{K}\right)\left(1 - \frac{u(\ell/2)}{K}\right)u(\ell/2),$$

which is negative for $u(\ell/2) > K/2$.

LEMMA 4.5. *Nontrivial stationary solutions of the critical patch-size problem are plateaus iff* $u(\ell/2) > K/2$.

4.3. Chemotaxis. The oriented movement of cells along chemical gradients is an important feature of all living organisms. It occurs, for example, in the development of embryos or for immune cell guidance toward an inflammation. In particular, cell-cell aggregations have been studied, where the attracting signal is released by the cells themselves. The mathematical analysis of chemotaxis models over the last 30 years has brought interesting results on finite time blow-up solutions and on pattern formation. We will recall some of these results and relate them to our classification of spikes and plateaus. It turns out that spikes are typical in the blow-up scenario, while plateaus are typical for global existence.

4.3.1. The Classical Chemotaxis Model. In one dimension the classical chemotaxis model reads in its easiest form [7]

$$\begin{aligned} u_t &= \Delta u - \nabla(\chi u \nabla v), \\ v_t &= D\Delta v + \alpha u - \beta v, \end{aligned} \tag{4.6}$$

where u denotes the cell density and v the concentration of the attractive signal. It is known that this model has finite time blow-up solutions in two or more spatial dimensions (see the review article of Horstmann [8]). In one dimension it has been shown in [10] and [7] that solutions exist globally in time and that patterns typically look like spike solutions. To confirm this within our classification we assume that, at steady state, u and v have a common maximum at x_0 such that

$$u'(x_0) = 0, \quad v'(x_0) = 0, \quad u''(x_0) < 0, \quad v''(x_0) < 0.$$

Thus from (4.6) we find

$$\begin{aligned} u^{\mathrm{IV}} &= \chi(u'''v' + 3u''v'' + 3u'v''' + uv^{\mathrm{IV}}), \\ Dv^{\mathrm{IV}} &= \beta v'' - \alpha u'', \end{aligned} \tag{4.7}$$

which evaluated at x_0 gives

$$\begin{aligned} u^{\mathrm{IV}}(x_0) &= \chi\big(3u''(x_0)v''(x_0) + u(x_0)v^{\mathrm{IV}}(x_0)\big), \\ v^{\mathrm{IV}}(x_0) &= \beta v''(x_0) - \alpha u''(x_0). \end{aligned} \tag{4.8}$$

For the second derivatives at x_0, we find from (4.6)

$$\begin{aligned} u''(x_0) &= \chi u(x_0)v''(x_0), \\ v''(x_0) &= \beta v(x_0) - \alpha u(x_0). \end{aligned}$$

Since we assume $v''(x_0) < 0$ we find

$$u(x_0) > \frac{\beta}{\alpha}\, v(x_0).$$

Using these relations, we observe from the second equation of (4.8) that

$$v^{\mathrm{IV}}(x_0) = (\beta - \alpha\chi u(x_0))v''(x_0),$$

which is positive for $u(x_0) > \frac{\beta}{\alpha\chi}$. Then $v(x_0)$ is a spike and consequently from (4.8) so is $u(x_0)$.

LEMMA 4.6. *Local maxima x_0 of steady state solutions of* (4.6) *in one dimension that satisfy $u(x_0) > \frac{\beta}{\alpha\chi}$ are spikes.*

The ratio $\beta/(\alpha\chi)$ has another meaning for the model above. Consider a spatially homogeneous steady state $\bar{u}(x) = \text{const}$ with $M := \int_\Omega \bar{u}(x)dx$. Then for the steady state $\bar{u}$ to be linearly unstable we necessarily need [12]

$$M > \frac{\beta}{\alpha\chi},$$

otherwise no pattern formation would be observed. In [7] we used asymptotic methods and showed that for $D \ll 1$ the value at the maximum is given as

$$u(x_0) \approx \frac{\chi^2 M^2}{2\alpha}.$$

Hence this maximum is a spike if $\frac{\chi^2 M^2}{2\alpha} > \frac{\beta}{\alpha\chi}$ or, equivalently, if $M > \sqrt{\frac{2\beta}{\chi^3}}$.

4.3.2. The Volume-Filling Chemotaxis Model. The volume-filling chemotaxis model, as introduced by Hillen and Painter [5, 12], includes the finite, nonzero volume of individual cells. In its simplest form it reads

$$\begin{aligned} u_t &= \Delta u - \nabla\big(\chi u(1-u)\nabla v\big), \\ v_t &= D\Delta v + \alpha u - \beta v. \end{aligned} \tag{4.9}$$

It was shown in [5] that solutions to this model exist globally in time for all space dimensions. Moreover, plateau solutions are typical steady states. We confirm this in one dimension and assume that u and v have a common maximum at x_0 such that

$$u'(x_0) = 0, \quad v'(x_0) = 0, \quad u''(x_0) < 0, \quad v''(x_0) < 0.$$

For steady states of (4.9) we find

$$\begin{aligned} u'' &= \chi\big((1-2u)u'v' + (u-u^2)v''\big), \\ Dv'' &= \beta v - \alpha u \end{aligned}$$

and

$$\begin{aligned} u^{\mathrm{IV}} = \chi\big(&- 4u'u''v' - 2u'^2 v'' - 2u'(u''v' + 2u'v'')\big) \\ &+ (1-2u)(u'''v' + u''v' + 2u''v'' + 2u'v''') \\ &+ (1-2u)u'v''' + (u-u^2)v^{\mathrm{IV}}, \\ Dv^{\mathrm{IV}} = \beta v'' - \alpha u''. \end{aligned}$$

We then find

$$u''(x_0) = \chi(u-u^2)v''(x_0), \tag{4.10}$$

$$Dv''(x_0) = \beta v(x_0) - \alpha u(x_0), \tag{4.11}$$

$$u^{\mathrm{IV}}(x_0) = \chi\big((1-2u)(3u''v'') + (u-u^2)v^{\mathrm{IV}}\big), \tag{4.12}$$

$$Dv^{\mathrm{IV}}(x_0) = \big(\beta - \alpha\chi(u-u^2)\big)v'', \tag{4.13}$$

where all functions are evaluated at $x = x_0$. We substitute (4.10) and (4.13) into (4.12) to obtain

$$u^{\mathrm{IV}} = \chi(u-u^2)\left(3\chi(1-2u)(v'')^2 + \frac{1}{D}(\beta - \alpha\chi(u-u^2))v''\right).$$

From the general existence result of [5], we know that $0 \le u \le 1$. In addition we assumed $v''(x_0) < 0$. Hence, if $u(x_0)$ is large enough such that

$$(1-2u) < 0 \quad \text{and} \quad \beta - \alpha\chi(u-u^2) > 0,$$

then $u^{\mathrm{IV}}(x_0) < 0$. This is true for

$$u(x_0) \ge u^*$$

with

$$u^* = \begin{cases} \frac{1}{2} + \frac{1}{2}\sqrt{1 - \frac{4\beta}{\alpha\chi}} & \text{if } \frac{4\beta}{\alpha\chi} \le 1, \\ \frac{1}{2} & \text{otherwise.} \end{cases} \tag{4.14}$$

LEMMA 4.7. *Local maxima x_0 of steady state solutions of the volume-filling chemotaxis model* (4.9) *in one dimension with $u(x_0) > u^*$ are plateaus.*

4.3.3. Chemotaxis with Finite Sampling Radius. Our last example related to chemotaxis is a model that includes a nonlocal gradient. This is used to model the fact that cells measure chemical signals via receptors that are attached to the cell membrane. In [6] we included this effect into chemotaxis models as

$$\begin{aligned} u_t &= \Delta u - \nabla\big(\chi u(1-u)\,\mathring{\nabla}_\rho\, v\big), \\ v_t &= D\Delta v + \alpha u - \beta v. \end{aligned} \tag{4.15}$$

We showed in [6] that solutions exist globally in time in all space dimensions and we constructed approximative plateau steady states.

4.4. The Gierer–Meinhardt Model. For a Gierer–Meinhardt model with saturation effects we study the specific problem of the stability of two-dimensional stripe patterns. Two-dimensional stripe patterns were studied in great detail in Kolokolnikov et al. [9]. The authors distinguished two types of stripe patterns, depending on the cross-sectional profile. For *homoclinic stripes* the cross-sectional profile is given by a homoclinic solution of an associated semilinear elliptic equation, whereas *mesa-stripes* have a cross section that can be approximated by two heteroclinic solutions that are "glued together" at the maximum. For the time evolution of stripes the authors classified three types of instabilities: (i) breakup instabilities, where the stripe breaks up into spots; (ii) zig zag instabilities, where the stripe deforms and starts a labyrinthian pattern; and (iii) pulse splitting instabilities, where the stripe splits up into two parallel stripes. In [9] they showed that some homoclinic stripes show breakup instabilities, while mesa-stripes have no such instabilities. They suggested that the "stability properties of 'fat' homoclinic stripes can be similar to those of mesa-stripe solutions...where spot generating breakup instabilities do not occur" [9, p. 17]. Using the classification of spikes and plateaus we will confirm this conjecture.

For the two unknown functions $a(x,t), h(x,t)$ with $x \in \mathbb{R}^2$ the Gierer–Meinhardt model with saturation reads

$$\begin{aligned} a_t &= \varepsilon^2 \Delta a - a + \frac{a^2}{h(1+ka^2)}, \\ \tau h_t &= D\Delta h - h + \frac{a^2}{\varepsilon}, \end{aligned} \tag{4.16}$$

where k denotes a bifurcation parameter. For $k = 0$ we get the Gierer–Meinhardt model without saturation. In that case there are only homoclinic stripes and these show breakup instabilities [9]. If k is positive but small, there still exist homoclinic stripes with breakup instabilities. As k reaches a threshold $k_0 > 0$ the homoclinic stripes become mesa-stripes which have no breakup instabilities. In [9] a scaling constant $\mathcal{H}$ is introduced that represents the height of the maximum of the stripe. This constant is used to rescale the bifurcation parameter as $b = k\mathcal{H}^2$. To compare our results with [9] we use the same notation here. They showed that mesa-stripes occur for $b > b_0 = 0.211376$ and that these have no breakup instabilities. Here we will show the following theorem.

THEOREM 4.8. *Let $0 \le b < b_0$. If the profile of the homoclinic stripe is a plateau, then there is no breakup instability. The threshold b_0 can be sharpened to $b_0^* = 0.196162$.*

Proof. For this proof we make extensive use of the results and methods from [9]. In [9] it is shown that the profile of a homoclinic stripe is given by the corresponding shadow equation for $w(y)$, where $y = x_1/\varepsilon$ and x_1 denotes the first component of $x \in \mathbb{R}^2$. The shadow system reads

$$w'' = f(w), \quad f(w) = w - \frac{w^2}{1+bw^2}, \quad -\infty < y < \infty. \tag{4.17}$$

Note that for a classification of spikes or plateaus the spatial scale, y or x_1, is irrelevant.

Equation (4.17) can be analyzed by writing it as a first order system for (w, w'). For $0 \le b < 1/4$ we obtain three equilibria: $(0,0)$ and $(w_\pm, 0)$ with

$$w_\pm = \frac{1}{2b}\left(1 \pm \sqrt{1-4b}\right)$$

(note that the b in the denominator is missing in formula (2.25) in [9]). Linear analysis shows that $(0,0)$ and $(w_+,0)$ are saddle points, while $(w_-,0)$ is a center. Moreover, the system for (w,w') has a Hamiltonian

$$\begin{aligned} H(w,w') &= \frac{(w')^2}{2} - \int_0^w f(s)ds \\ &= \frac{(w')^2}{2} - \frac{w^2}{2} - \frac{\pi}{2b\sqrt{b}} + \frac{1}{b\sqrt{b}} \tan^{-1}\left(\frac{1}{w\sqrt{b}}\right). \end{aligned}$$

It was shown in [9] that a homoclinic solution originating at $(0,0)$ exists for all $0 < b < b_0 = 0.211376$. Since the Hamiltonian is constant along trajectories, a homoclinic orbit originating at $(0,0)$ has energy $H(0,0) = 0$. Let $\bar{w}$ denote the unique intersection of the homoclinic orbit with the w-axis. By symmetry we have $w(0) = \bar{w}$ and also $w_- < \bar{w} < w_+$. Moreover, $\bar{w}$ is a local maximum of the homoclinic connection. From $H(\bar{w}, 0) = 0$ we obtain after minor rearrangements

$$-b\bar{w}^2 + 2\bar{w} - \frac{\pi}{\sqrt{b}} + \frac{2}{\sqrt{b}} \tan^{-1}\left(\frac{1}{\bar{w}\sqrt{b}}\right) = 0. \tag{4.18}$$

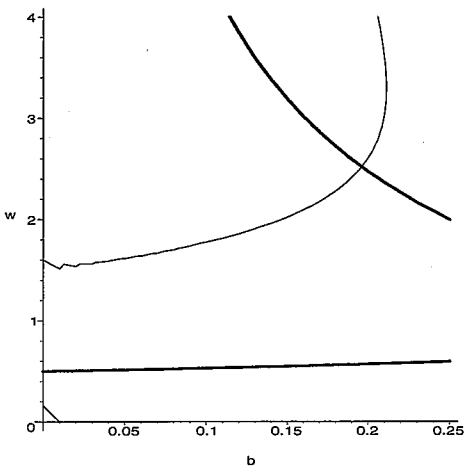

Fig. 5 *The thick solid curve shows* (4.19) *and the thin solid line shows* (4.18) *in a* (b,w)*-diagram. We see clearly a unique intersection at* $(b_0^*,\bar{w})$*. For* $b > b_0$ *there is no solution of* (4.18).

Next we investigate the spike/plateau structure of the homoclinic solution $w(y)$. From (4.17) we find that

$$w^{IV} = f''(w)w'^2 + f'(w)w''.$$

At the maximum $y = 0$ we obtain

$$w^{IV}(0) = f'(\bar{w})w''(0).$$

Since $y = 0$ is a maximum we have $w''(0) < 0$. Hence 0 is a spike for $f'(\bar{w}) < 0$ and a plateau for $f'(\bar{w}) > 0$. It is straightforward to check that $f'(w_-) < 0$ and $f'(w_+) > 0$. Hence if $\bar{w}$ is close to w_-, the homoclinic solution is a spike, and if $\bar{w}$ is close to w_+, it is a plateau. Moreover, it was shown in [9] that $\lim_{b\to 0}\bar{w} = w_-$ and $\lim_{b\to b_0}\bar{w} = w_+$. In addition $f'(\bar{w})$ is monotonically increasing in b. Hence there is a unique b_0^* such that

$$f'(\bar{w}) = 0,$$

which can be rewritten as

$$(1 + b_0^*(\bar{w})^2)^2 = 2\bar{w}. \tag{4.19}$$

With (4.18) and (4.19) we have two equations for two unknowns $(b_0^*,\bar{w})$. We use Maple to solve these equations to get

$$b_0^* = 0.1961626842, \qquad \bar{w} = 2.518679189.$$

In Figure 5 we plot the two curves (4.18) and (4.19) that have a unique intersection.

LEMMA 4.9. *Let* $0 < b < b_0$. *If* $0 < b < b_0^*$, *the homoclinic connection of* (4.17) *is a spike and for* $b_0^* < b < b_0$ *it is a plateau.*

In a last step we show that plateau-stripes cannot have breakup instabilities. In "Principal result 2.6" of [9] the existence of breakup instabilities on an $O(1)$ timescale is linked to the existence of a positive eigenvalue of an operator L_{0b} defined as

$$L_{0b}\Phi := \Phi'' - \Phi + \frac{2w}{(1+bw^2)^2}\Phi,$$

which we write as

$$L_{0b}\Phi = \Phi'' - f'(w)\Phi.$$

For a plateau we have $f'(\bar{w}) > 0$, and hence in that case L_{0b} cannot have a positive eigenvalue. This implies, according to [9, section 2.3], that there exists no breakup instability. □

4.5. The Gray–Scott Model. Hale, Peletier, and Troy [3] calculated exact homoclinic and heteroclinic steady state solutions for a Gray–Scott model with autocatalysis. After nondimensionalization the model reads

$$\begin{aligned} u_t &= u_{xx} - uv^2 + \lambda(1-u), \\ v_t &= \gamma v_{xx} + uv^2 - v, \end{aligned} \tag{4.20}$$

where λ and γ are two model parameters. For the steady state analysis Hale, Peletier, and Troy assumed that

$$\lambda\gamma = 1 \qquad \text{and} \qquad 0 < \gamma < \frac{1}{4}. \tag{4.21}$$

In [3] they explicitly constructed the following homoclinic and heteroclinic solutions $(u(x), v(x))$.

LEMMA 4.10 (Theorems A and B from [3]). *Let γ and λ satisfy* (4.21).

(a) *If $0 < \gamma < \frac{2}{9}$, then there exists a homoclinic pulse*

$$u(x) = 1 - \frac{3\gamma}{1 + Q\cosh(x/\sqrt{\gamma})}, \quad v(x) = \frac{3}{1 + Q\cosh(x/\sqrt{\gamma})},$$

with $Q = \sqrt{1 - 9\gamma/2}$.

(b) *If $\frac{2}{9} < \gamma < \frac{1}{4}$, there exists a homoclinic pulse*

$$u(x) = \frac{1-\omega}{2} + \frac{a\gamma}{1 + b\cosh(cx)}, \quad v(x) = \frac{1+\omega}{2\gamma} - \frac{a}{1 + b\cosh(cx)},$$

with

$$a = \frac{3\omega(1+\omega)}{\gamma(1+3\omega)}, \; b = \frac{\sqrt{1-3\omega}}{1+3\omega}, \; c = \frac{\sqrt{\omega(1+\omega)}}{\gamma\sqrt{2}}, \; \omega = \sqrt{1-4\gamma}. \tag{4.22}$$

(c) *For $\gamma = \frac{2}{9}$ there exists a heteroclinic steady state*

$$u(x) = \frac{1}{3}\left\{2 - \tanh\left(\frac{3x}{2\sqrt{2}}\right)\right\}, \quad v(x) = \frac{3}{2}\left\{1 + \tanh\left(\frac{3x}{2\sqrt{2}}\right)\right\}.$$

Note that in all cases a maximum of $u(x)$ corresponds to a minimum of $v(x)$, and vice versa.

From the heteroclinic solution of case (c) we can construct a local maximum by gluing together two $\tanh(3x/(2\sqrt{2}))$ functions, much like for the Cahn–Hilliard solution in (4.2) with $\varepsilon = 2\sqrt{2}/3 \approx 0.9428$. As before it can be shown that this solution is of plateau type.

Next we study the spike/plateau properties of the homoclinic solutions of cases (a) and (b) of Lemma 4.10.

THEOREM 4.11. *There exist values* $\gamma_1^*, \gamma_2^* > 0$ *with* $0 < \gamma_1^* < \frac{2}{9} < \gamma_2^* < \frac{1}{4}$ *such that the solution of Lemma* 4.10 *is a spike for* $\gamma \in (0, \gamma_1^*) \cup (\gamma_2^*, \frac{1}{4})$ *and a plateau for* $\gamma \in (\gamma_1^*, \gamma_2^*)$. *The values can be computed as*

$$\gamma_1^* = \frac{24}{25}\frac{2}{9}, \qquad \gamma_2^* = \frac{1-(\omega^*)^2}{4}, \quad \omega^* = \frac{1}{2}\sqrt{\frac{275}{3}} - \frac{9}{2},$$

which gives approximately

$$\gamma_1^* = 0.21\bar{3}, \qquad \gamma_2^* = 0.22938.$$

Proof. The homoclinic solutions of Lemma 4.10 show their x-dependence in a term of the form

$$\frac{\alpha}{1+\beta\cosh cx};$$

since the classification is scale invariant we set $y = cx$ and study

$$g(y) := \frac{\alpha/\beta}{1/\beta + \cosh(y)} = \frac{A}{B+\cosh(y)}.$$

We compute for the maximum at $y = 0$,

$$g^{IV}(0) = \frac{A}{(B+1)^3}(5-B).$$

Hence 0 is a spike for $B < 5$ and a plateau for $B > 5$.

In case (a) of Lemma 4.10 we have $B = \frac{1}{Q}$ and $Q = \sqrt{1-9\gamma/2}$. Hence the threshold for γ corresponding to the case $B = 5$ is given by $\gamma_1^* = \frac{24}{25}\frac{2}{9}$.

In case (b) of Lemma 4.10 we have $B = \frac{1}{b}$, where b is given in (4.22). Here the critical case of $B = 5$ corresponds to $\gamma_2^* = \frac{1-(\omega^*)^2}{4}$, where ω^* is the positive solution of the quadratic $(\omega^*)^2 + 9\omega^* - \frac{8}{3} = 0$. □

5. Discussion. In this paper we give a simple classification of spikes and plateaus using fourth order derivatives. We show that this classification can be used for the qualitative analysis of complicated PDEs and in many cases the stability properties of spikes and plateaus are different. I expect that many more useful applications of this classification can be found.

For further studies it would be interesting to understand $\mathrm{Hess}(\Delta u)$ from the point of view of differential geometry. Maybe the trace of a fourth order derivative has a specific geometric meaning and can be used to classify extremal points of surfaces or general manifolds.

REFERENCES

[1] N. ALIKAKOS, P.W. BATES, AND P. FUSCO, *Slow motion for the Cahn–Hilliard equation in one space dimension*, J. Differential Equations, 90 (1991), pp. 81–135.

[2] G. DE VRIES, T. HILLEN, M. LEWIS, J. MÜLLER, AND B. SCHÖNFISCH, *A Course in Mathematical Biology*, SIAM, Philadelphia, 2006.

[3] J.K. HALE, L.A. PELETIER, AND W.C. TROY, *Exact homoclinic and heteroclinic solutions of the Gray–Scott model for autocatalysis*, SIAM J. Appl. Math., 61 (2000), pp. 102–130.

[4] T. HILLEN, *On the L^2-closure of transport equations: The general case*, Discrete Contin. Dyn. Syst. Ser. B , 5 (2005), pp. 299–318.

[5] T. HILLEN AND K. PAINTER, *Global existence for a parabolic chemotaxis model with prevention of overcrowding*, Adv. Appl. Math., 26 (2001), pp. 280–301.

[6] T. HILLEN, K. PAINTER, AND C. SCHMEISER, *Global existence for chemotaxis with finite sampling radius*, Disc. Cont. Dyn. Syst. B, 7 (2007), pp. 125–144.

[7] T. HILLEN AND A. POTAPOV, *The one-dimensional chemotaxis model: Global existence and asymptotic profile*, Math. Meth. Appl. Sci., 27 (2004), pp. 1783–1801.

[8] D. HORSTMANN, *From* 1970 *until present: The Keller-Segel model in chemotaxis and its consequences* I, Jahresber. Deutsch. Math.-Verein., 105 (2003), pp. 103–165.

[9] T. KOLOKOLNIKOV, W. SUN, M. WARD, AND J. WEI, *The stability of a stripe for the Gierer–Meinhardt model and the effect of saturation*, SIAM J. Appl. Dyn. Syst., 5 (2006), pp. 313–363.

[10] K. OSAKI AND A. YAGI, *Finite dimensional attractor for one-dimensional Keller-Segel equations*, Funkcial. Ekvac., 44 (2001), pp. 441–469.

[11] H.G. OTHMER AND T. HILLEN, *The diffusion limit of transport equations* II: *Chemotaxis equations*, SIAM J. Appl. Math., 62 (2002), pp. 1222–1250.

[12] K. PAINTER AND T. HILLEN, *Volume-filling and quorum-sensing in models for chemosensitive movement*, Can. Appl. Math. Q., 10 (2002), pp. 501–543.

[13] V.M. TIKHOMIROV, *Selected Works of A.N. Kolmogorov*, Kluwer Academic, Dordrecht, The Netherlands, 1991.

[14] M. WARD AND J. WEI, *Hopf bifurcation and oscillatory instabilities of spike solutions for the one-dimensional Gierer–Meinhardt model*, J. Nonlinear Sci., 13 (2003), pp. 209–264.